



Anatomical implication of less occurrence of inferior oblique muscle entrapment in orbital floor trapdoor fracture

Shinjiro Kono¹ · Aric Vaidya^{1,2} · Hidetaka Miyazaki¹ · Hirohiko Kakizaki¹ · Yasuhiro Takahashi¹

Received: 9 June 2021 / Accepted: 23 July 2021 / Published online: 27 July 2021
© The Author(s), under exclusive licence to Springer-Verlag France SAS, part of Springer Nature 2021

Abstract

Purpose To examine the anatomy of the inferior oblique (IO) muscle and its surrounding structures to clarify why IO muscle entrapment develops less in orbital floor trapdoor fractures.

Methods Computed tomographic (CT) images on the unaffected sides were obtained from 64 patients with unilateral orbital fractures. On coronal planes, presence or absence of an infraorbital groove below the IO muscle was confirmed. At the level of the medial margin of the infraorbital groove/canal, the distance from the orbital floor to the IO muscle (IO-floor distance), the thickness of the orbital floor, and the shortest distance from the inferior rectus (IR) muscle to the orbital floor (shortest IR-floor distance) were measured. On quasi-sagittal planes, the distances from the inferior orbital rim to the inferior margin of the IO muscle (IO-rim distance) and the most anterior point of the infraorbital groove (groove-rim distance) were measured.

Results The infraorbital groove was found below the IO muscle in eight patients (12.5%), and the IO-rim and IO-floor distances were significantly longer than the groove-rim and shortest IR-floor distances, respectively ($p < 0.001$). The orbital floor below the IO muscle was significantly thicker than that below the IR muscle ($p < 0.001$).

Conclusion Although the medial margin of the infraorbital groove is the most common fracture site, the IO muscle was not located above the groove in most cases. A longer IO-floor distance and thicker orbital floor below the IO muscle may also contribute to less occurrence of IO muscle entrapment in orbital floor trapdoor fractures.

Keywords Inferior oblique muscle · Inferior rectus muscle · Infraorbital groove · Orbital floor trapdoor fracture

Introduction

Orbital trapdoor fracture is one of the types of orbital fracture that frequently occurs in the pediatric age group [10, 13, 16]. After the displacement of the fractured bone with a hinge, the bone easily snaps back and returns to the original position due to the high elasticity of the bone [10, 13, 16]. In such situations, the orbital tissues are incarcerated at the fracture site. The orbital floor is more frequently involved, while trapdoor fracture in the medial orbital wall is less common [13]. In orbital floor trapdoor fractures, a fracture line usually runs along the medial margin of the infraorbital

groove as this part is anatomically vulnerable to blunt ocular trauma [11, 16].

The inferior rectus (IR) muscle, medial rectus muscle, orbital fat, and inferior oblique (IO) muscle branch of the oculomotor nerve are commonly incarcerated orbital tissues because these are located close to the orbital floor/medial orbital wall [13, 16]. On the contrary, there had been only two reported cases of orbital fracture with IO muscle entrapment [3, 6], nevertheless the IO muscle also runs close to the orbital floor [1, 14].

We examined the anatomical relationship between the IO muscle and infraorbital groove using computed tomographic (CT) images to elucidate why IO muscle entrapment occurs less in orbital floor trapdoor fractures.

✉ Yasuhiro Takahashi
yasuhiro_tak@yahoo.co.jp

¹ Department of Oculoplastic, Orbital and Lacrimal Surgery, Aichi Medical University Hospital, 1-1 Yazako-Karimata, Nagakute, Aichi 480-1195, Japan

² Department of Oculoplastic, Orbital and Lacrimal Surgery, Rapti Eye Hospital, Dang, Nepal

Methods

Study design

This study was a retrospective chart review of consecutive Japanese patients with an orbital fracture in whom CT was taken before and 1 day after surgical reduction between January 2020 and May 2021 (Fig. 1). Patients with missing data, those with a bilateral orbital fracture, and those with orbital rim involvement were excluded from this study.

Data collection

The data on age, sex, and fracture side were collected from the medical charts of all the patients. Fracture sites, presence or absence of trapdoor fracture, incarcerated tissues in trapdoor fracture were confirmed using preoperative CT images. Extraocular muscle entrapment was defined by the following CT findings: a minimally displaced orbital fracture and missing rectus [16]. We did not check for the incarceration of the IO muscle branch of the oculomotor nerve because we did not review the IO muscle under-action on the Hess chart.

Measurements on CT

Contiguous 1 mm axial, coronal, and quasi-sagittal (parallel to the optic nerve) CT images (Aquilion Precision, Canon, Tokyo, Japan, or SOMATOM AS plus, Siemens Japan K.K., Tokyo, Japan) were obtained (75–100 mAs, 120 kV, slice

thickness, 1 mm, pitch 0.638 or 0.8, collimation, 0.5 or 0.6, matrix. 512×512, field of view, 150–200 mm) using bone window algorithms (window level, 500–600, window width 2500). The unaffected sides were used for measurements. All measurements were performed using the digital caliper and the freehand measuring tools of the image viewing software (ShadeQuest/ViewR, Yokogawa Medical Solutions Corporation, Tokyo, Japan) by one of the authors (YT).

On coronal planes, the presence or absence of the infraorbital groove below the IO muscle was confirmed (Fig. 2a to c). The infraorbital groove has a bony defect above the infraorbital nerve, while the infraorbital canal consists of a complete cylinder-shaped bone [11]. In a few cases, although the infraorbital groove did not have the bony defect, we distinguished the infraorbital groove from the canal when the medial wall of the groove inclined from the superomedial to inferolateral direction [11].

In orbital floor trapdoor fractures, since a fracture line usually runs along the medial margin of the infraorbital groove [11, 16], the points just medial to the infraorbital groove and canal were used as the reference points for measurement of the following distances and thicknesses. The distance from the inferior margin of the IO muscle to the infraorbital groove/canal (IO-floor distance) and the thickness of the orbital floor at the same point were measured (Fig. 2b, c). The distance between the inferior margin of the IR muscle and the most anterior part of the infraorbital groove (IR-floor distance) and the thickness of the orbital floor at the same point were also measured (Fig. 2d, e). Also, the shortest distance from the inferolateral margin of the IR

Fig. 1 A flowchart of patient inclusion and grouping

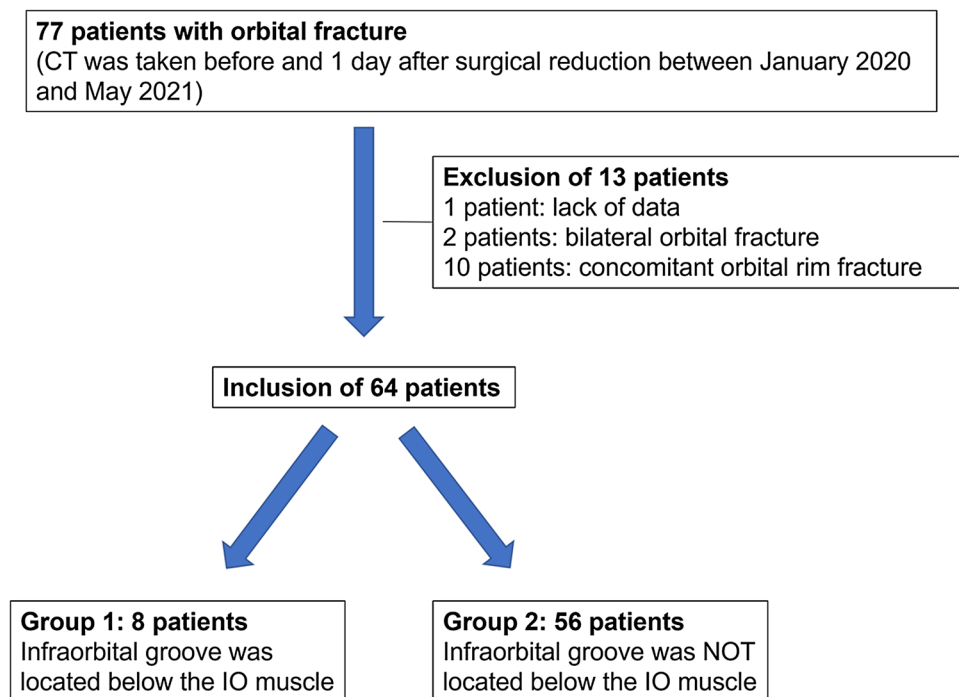




Fig. 2 Measurements on computed tomographic (CT) images. The window level and width were intentionally changed in all figures except Fig. 2g for clear depiction of both the muscles and bone, but actual measurements were performed on CT images with bone window algorithms. **a** Presence of the infraorbital groove below the inferior oblique (IO) muscle. **b, c** Measurements of the distance from the inferior margin of the IO muscle to the orbital floor and thickness of the orbital floor at the level of the medial margin of the infraorbital canal. **b** is a magnified image of the measurement area. **d, e** Measure-

ments of the distance from the inferior margin of the inferior rectus (IR) muscle to the orbital floor and thickness of the orbital floor at the level of the medial margin of the infraorbital groove. **d** is a magnified image of the measurement area. **f** Measurements of the distances from the inferior orbital rim to the posterior margin of the IO muscle (yellow solid line and pink solid arrow) and to the anterior margin of the infraorbital groove (yellow broken line and pink broken arrow). **g** Measurement of the anterior globe position. **h** Measurement of the anteroposterior orbital length

muscle to the infraorbital groove (shortest IR-floor distance) was measured.

On the quasi-sagittal plane showing the infraorbital groove, the distances from the inferior orbital rim to the vertical line through the posterior margin of the IO muscle (IO-rim distance) and to the most anterior point of the infraorbital groove (groove-rim distance) were measured (Fig. 2f).

On the axial plane showing the optic nerve, the distance from the top of the cornea to the interzygomatic line was measured for evaluating the anterior globe position (Fig. 2g) [9]. On the sagittal plane showing the optic nerve, the distance from the inferior orbital rim to the orbital process of

the palatal bone was measured for evaluating the anteroposterior orbital length (Fig. 2h) [15].

Statistical analysis

Patient age and measurement results were expressed as means \pm standard deviations. The differences between the IO-floor and IR-floor distances, the IO-floor and shortest IR-floor distances, the thickness of the orbital floor below the IO and IR muscles, and the IO-rim and groove-rim distances were analyzed using the Student's *t* test. The measurement values were compared between the patients with (Group 1) and without (Group 2) the infraorbital groove located below

the IO muscle using the Mann–Whitney U test. All statistical analyses were performed using SPSS™ ver. 26 software (IBM Japan, Tokyo, Japan). A p value of <0.05 was considered statistically significant.

Results

Surgical reduction of orbital fracture was performed in 77 patients, but 13 patients were excluded from this study because of the lack of data (two patients), bilateral orbital fracture (one patient), or concomitant orbital rim involvement (10 patients) (Fig. 1). This study included 64 sides from 64 patients with an orbital fracture. Patient demographic data are shown in Table 1.

The results of measurements and statistical analyses are shown in Tables 2 and 3. The IO-floor distance was not significantly different from the IR-floor distance ($p=0.180$). However, the IO muscle was significantly farther from the orbital floor, compared with the IR muscle at the closest point to the orbital floor (shortest IR-floor distance) ($p<0.001$). The orbital floor below the IO muscle was significantly thicker than that below the IR muscle ($p<0.001$). The IO-rim distance was significantly longer compared with the groove-rim distance ($p<0.001$).

The infraorbital groove was found to be located below the IO muscle in eight patients (group 1, 12.5%). Six of the eight patients were 20 years old or younger, and the remaining two patients were 69 and 78 years old, respectively. The IO-floor distance tended to be shorter in group 1 than group 2 ($p=0.058$), while the IR-floor ($p<0.001$) and shortest IR-floor distances ($p=0.051$) tended to be longer in group 1 compared with group 2. The thickness of the orbital floor

Table 1 Patient demographic data

Number of patients (M/F)	64 (45/19)
Measurement sides (R/L)	37/27
Patient age (years)	35.1 ± 24.3
Fracture sites	
Right orbital floor	17
Right medial orbital wall	2
Right orbital floor + medial orbital wall	8
Left orbital floor	27
Left medial orbital wall	4
Left orbital floor + medial orbital wall	6
Trapdoor fracture	21 (32.8%)
Incarcerated tissues	
IR muscle	3
MR muscle	1
Orbital fat	17

M male, F female, R right, L left, IR inferior rectus, MR medial rectus

Table 2 Measurement results

Presence of infraorbital groove below inferior oblique muscle	8 (12.5%)
IO-floor distance (mm)	3.16 ± 1.15
IR-floor distance (mm)	2.85 ± 1.41
p value	0.180
Shortest IR-floor distance (mm)	0.72 ± 0.66
p value (vs. IO-floor distance)	<0.001
Thickness of orbital floor (mm)	
Below IO muscle	1.97 ± 0.85
Below IR muscle	1.43 ± 0.47
p value	<0.001
IO-rim distance (mm)	7.59 ± 2.16
Groove-rim distance (mm)	11.61 ± 2.93
p value	<0.001
Anterior globe position (mm)	16.79 ± 3.06
Anteroposterior orbital length (mm)	38.24 ± 3.59

IO inferior oblique, IR inferior rectus

below the IO muscle was significantly thinner in group 1 ($p=0.015$). The IO-rim distance was longer than the groove-rim distance in group 1, while the groove-rim distance was longer than the IO-rim distance in group 2 ($p<0.001$). Although the anteroposterior orbital length was not significantly different between the groups ($p=0.405$), the anterior globe position was significantly less prominent in group 1 ($p=0.002$).

Discussion

The anatomy of the IO muscle and its surrounding structures was examined for elucidating the less occurrence of IO muscle incarceration at the site of orbital floor trapdoor fracture.

Orbital floor trapdoor fractures usually occur along the medial margin of the infraorbital groove [13, 16]. However, in this study, the inferior margin of the IO muscle was located above the infraorbital groove in only 12.5% of patients, and the IO-rim distance was significantly shorter than the groove-rim distance. These results indicate that the IO muscle frequently lies away from the most common site of fracture.

The IO muscle originates from the orbital floor just lateral to the entrance of the nasolacrimal canal and runs obliquely in the superolateral direction toward the globe [1, 14]. The anteromedial part of the IO muscle is, therefore, located close to the orbital floor. However, the most anterior point of the infraorbital groove is located slightly laterally in the orbital floor. In this study, the IO muscle was found to run approximately 3 mm above the orbital floor at the level of the infraorbital groove/canal, and the IO-floor distance was significantly longer than the shortest IR-floor distance. These

Table 3 Comparison of measurement results between the groups

	Group 1: presence of infraorbital groove below IO muscle ($n=8$)	Group 2: absence of infraorbital groove below IO muscle ($n=56$)	<i>p</i> value
Age (years)	29.8 ± 27.6	35.9 ± 24.0	0.529
IO-floor distance (mm)	2.52 ± 1.35	3.25 ± 1.10	0.058
IR-floor distance (mm)	5.11 ± 0.88	2.53 ± 1.16	<0.001
Shortest IR-floor distance (mm)	1.10 ± 0.36	0.66 ± 0.68	0.051
Thickness of orbital floor (mm)			
Below IO muscle	1.41 ± 0.37	2.05 ± 0.87	0.015
Below IR muscle	1.41 ± 0.37	1.44 ± 0.48	0.768
IO-rim distance (mm)	10.05 ± 1.21	7.24 ± 2.03	<0.001
Groove-rim distance (mm)	7.68 ± 1.37	12.17 ± 2.65	<0.001
Anterior globe position (mm)	13.81 ± 1.31	17.22 ± 3.00	0.002
Anteroposterior orbital length (mm)	37.52 ± 3.73	38.34 ± 3.60	0.405

IO inferior oblique, IR inferior rectus

findings imply less possibility of IO muscle incarceration compared with the IR muscle.

The orbital floor below the IO muscle was significantly thicker than that below the IR muscle. This also reduces the risk of IO muscle entrapment.

Group 1 showed a less prominent anterior globe position compared with group 2. In the less proptotic patients, the IO muscle runs more posteriorly, resulting in the location of the IO muscle above the infraorbital groove. Two of the eight patients in group 1 were old, and old age people tend to show less amount of proptosis due to decreased amount of orbital fat [2]. However, in a previous study, older patients with trapdoor fracture had only orbital fat incarceration without extraocular muscle entrapment [13]. So, even in group 1, those older patients may have less risk of IO muscle incarceration. On the contrary, the remaining six patients in group 1 were 20 years old or younger. Young people tend to have less proptotic eyes [2] and high bone elasticity [13]. Moreover, patients in group 1 demonstrated a shorter IO-floor distance and a thinner orbital floor below the IO muscle than those in group 2. Such patients may have a risk of IO muscle entrapment.

In a previously reported case with IO muscle entrapment, the IR muscle and orbital fat were concomitantly incarcerated [6]. The IO muscle shares a common fascial sheath with the IR muscle [7], and the extraocular muscles are connected with the orbital fat via the orbital connective tissue septal system [4]. Slippage of the IR muscle and orbital fat into the fracture site can drag the IO into the fracture site [6, 8, 11], resulting in IO muscle entrapment.

As similar to the IO muscle, the IO muscle branch of the oculomotor nerve is also farther from the infraorbital groove in the anterior orbit when compared to the IR muscle [1, 14]. However, this nerve is occasionally incarcerated in cases with orbital floor trapdoor fracture [5, 12]. In

a previous study, 18.6% of cases with orbital floor trapdoor fracture showed incarceration of the IO muscle branch [12]. Unlike the IO muscle, as the nerve has less tension, it may be more easily dragged by prolapsed orbital fat.

Incarceration of the IO muscle branch of the oculomotor nerve may be underestimated as such patients hardly notice diplopia, especially when they compensate it with head tilt. Furthermore, this is hardly detectable without Hess chart. However, incarceration of the IO muscle causes additional clinical signs, including nausea, vomiting, and bradycardia. Therefore, surgeons should elaborately examine patients with such signs not to overlook the IO muscle entrapment.

Our study was limited by several factors. First, this had a retrospective nature. Second, the inclusion of only Japanese patients was another limitation as the periocular anatomy has differences among populations [1]. Third, all the examinations were performed by a single clinician, which may cause an examiner bias.

In conclusion, we examined the anatomy of the IO muscle and its surrounding structures to clarify why the IO muscle has less risk of incarceration in orbital floor trapdoor fractures. The IO muscle was not located above the infraorbital groove in most of the cases, and a longer IO-floor distance and a thicker orbital floor below the IO muscle may also be the anatomical factors for less occurrence of IO muscle entrapment. On the contrary, some young patients with less proptotic eyes had the IO muscle located above the infraorbital groove, short IO-floor distance, and thin orbital floor. If orbital floor trapdoor fracture with the IR muscle and orbital fat incarceration occurs in such patients, the IO muscle can be entrapped. However, the low probability of this phenomenon is reflected by the only 2 reported cases with IO muscle entrapment, so far [3, 6].

Acknowledgements Other contributors: no one contributed to the work who did not meet our authorship criteria.

Author contributions SK manuscript writing. AV manuscript editing. HM manuscript editing. HK manuscript editing, supervision, and funding. YT protocol/project development, data collection, data analysis, and manuscript writing/editing.

Funding None.

Declarations

Conflicts of interests The authors declared no potential conflicts of interest with respect to the research, authorship, and/or publication of this article.

Ethical approval This study was approved by the Institutional Review Board (IRB) of our institution (No. 2021–40) and followed the tenets of the 1964 Declaration of Helsinki.

Consent to participate The IRB granted a waiver of informed consent for this study on the basis of the ethical guidelines for medical and health research involving human subjects established by the Japanese Ministry of Education, Culture, Sports, Science, and Technology and the Ministry of Health, Labour, and Welfare. The waiver was granted because the study was a retrospective review and not an interventional study and because it was difficult to obtain consent from patients who had been treated several years prior to this study. Nevertheless, at the request of the IRB, an outline of the study was published on the website of our institution and this was made available for public viewing. This public posting also gave patients an opportunity to decline participation, although no refusal was made known to us. Personal identifiers were removed from the records prior to data analysis.

Consent for publication All authors agreed with publication of this paper.

Data availability and material All data are included in this paper.

References

- Ana-Magadia MG, Valencia MRP, Naito M, Nakano T, Miyazaki H, Kakizaki H, Takahashi Y (2020) Location of the myoneural junction of the inferior oblique muscle: an anatomic study. *Ann Anat*. <https://doi.org/10.1016/j.aanat.2019.151429>
- Challa NK, Alghamdi WM (2021) Normal ocular protrusion values in South Indian population and effect of age, gender and refractive status on ocular protrusion. *Clin Ophthalmol* 15:1445–1451. <https://doi.org/10.2147/OPHTH.S302154>
- Kim S, Kim TK, Kim SH (2009) Clinicoradiologic findings of entrapped inferior oblique muscle in fracture of the orbital floor. *Korean J Ophthalmol* 23:224–227. <https://doi.org/10.3341/kjo.2009.23.3.224>
- Koornneef L (1977) New insights in the human orbital connective tissue: result of a new anatomical approach. *Arch Ophthalmol* 95:1269–1273. <https://doi.org/10.1001/archophth.1977.0445070167018>
- Lee JH, Shim HS, Woo KI, Kim YD (2013) Inferior oblique underaction: a transient complication related to inferior orbital wall fracture in childhood. *Acta Ophthalmol* 91:685–690. <https://doi.org/10.1111/j.1755-3768.2012.02466.x>
- Lee PAL, Kono S, Kakizaki H, Takahashi Y (2021) Entrapment of the inferior oblique and inferior rectus muscles in orbital trapdoor fracture. *Orbit*. <https://doi.org/10.1080/01676830.2021.1914669>
- Miller JM, Demer JL, Poukens V, Pavlovski DS, Nguyen HN, Rossi EA (2003) Extraocular connective tissue architecture. *J Vis* 3:240–251. <https://doi.org/10.1167/3.3.5>
- Nardi M (1996) Hypertropia and posterior blowout fracture. *Ophthalmology* 103:995–996. [https://doi.org/10.1016/s0161-6420\(96\)30550-2](https://doi.org/10.1016/s0161-6420(96)30550-2)
- Schmidt P, Kempin R, Langner S, Beule A, Kindler S, Koppe T, Völzke H, Ittermann T, Jürgens C, Tost F (2019) Association of anthropometric markers with globe position: a population-based MRI study. *PLoS ONE*. <https://doi.org/10.1371/journal.pone.0211817>
- Silverman N, Spindle J, Tang SX, Wu A, Hong BK, Shore JW, Wester S, Levin F, Connor M, Burt B, Nakra T, Shepler T, Hink E, El-Sawy T, Shinder R (2017) Orbital floor fracture with entrapment: Imaging and clinical correlations in 45 cases. *Orbit* 36:331–336. <https://doi.org/10.1080/01676830.2017.1337180>
- Takahashi Y, Nakano T, Miyazaki H, Kakizaki H (2016) An anatomical study of the orbital floor in relation to the infraorbital groove: implications of predisposition to orbital floor fracture site. *Graefes Arch Clin Exp Ophthalmol* 254:2049–2055. <https://doi.org/10.1007/s00417-016-3455-2>
- Takahashi Y, Sabundayo MS, Miyazaki H, Mito H, Kakizaki H (2017) Incarceration of the inferior oblique muscle branch of the oculomotor nerve in patients with orbital floor trapdoor fracture. *Graefes Arch Clin Exp Ophthalmol* 255:2059–2065. <https://doi.org/10.1007/s00417-017-3790-y>
- Takahashi Y, Sabundayo MS, Miyazaki MH, Kakizaki H (2018) Orbital trapdoor fractures: different clinical profiles between adult and paediatric patients. *Br J Ophthalmol* 102:885–891. <https://doi.org/10.1136/bjophthalmol-2017-310890>
- Tsutsumi S, Nakamura M, Tabuchi T, Yasumoto Y, Ito M (2013) An anatomic study of the inferior oblique nerve with high-resolution magnetic resonance imaging. *Surg Radiol Anat* 35:377–383. <https://doi.org/10.1007/s00276-012-1040-x>
- Vaidya A, Lee PAL, Kitaguchi Y, Kakizaki H, Takahashi Y (2020) Spontaneous orbital decompression in thyroid eye disease: new measurement methods and its influential factors. *Graefes Arch Clin Exp Ophthalmol* 258:2321–2329. <https://doi.org/10.1007/s00417-020-04762-0>
- Valencia MR, Miyazaki H, Ito M, Nishimura K, Kakizaki H, Takahashi Y (2021) Radiological findings of orbital blowout fractures: a review. *Orbit* 40:98–109. <https://doi.org/10.1080/01676830.2020.1744670>

Publisher's Note Springer Nature remains neutral with regard to jurisdictional claims in published maps and institutional affiliations.